JOURNAL OF MATERIALS SCIENCE 25 (1990) 4579–4586

Tensile flow and fracture behaviour of a superplastic Al–Ca–Zn alloy

K. SWAMINATHAN, K. A. PADMANABHAN
Department of Metallurgical Engineering, Indian Institute of Technology, Madras 600 036, India

The tensile flow behaviour in the range 275 to 550° C of an ultra-fine-grained superplastic Al–Ca–Zn alloy is reported. Under certain conditions of temperature and strain rate, superplastic ductility could be established. Fracture surfaces of tensile specimens tested in the above temperature range were examined by scanning electron microscopy and a correlation could be obtained between the ductility, as revealed by the tension tests, and the fracture behaviour. The fractographic studies also suggested a transition in the deformation process from grain deformation (mainly slip) at the lower temperatures to grain-boundary deformation (predominantly grain-boundary sliding) in the vicinity of 425° C.

1. Introduction

Moore and Morris [1] have reported structural superplasticity in an Al–Ca–Zn alloy and have also demonstrated its commercial potential by forming components of complex shapes and details. The above alloy had an ultra-fine grain size and medium strength and belongs to the group of superplastic alloys in which grain refinement is achieved through static recrystallization. Maximum elongation of about 900% under optimal conditions of temperature and strain rate has been achieved [2]. The room-temperature forming limit diagram and strain distribution under punch stretching of this alloy were reported earlier [3]. That study also considered the tensile flow behaviour from room temperature to 200° C.

In this paper, tensile flow behaviour at temperatures in the range 275 to 550° C and different strain rates are reported. Fractography, in terms of scanning electron microscopy (SEM), was resorted to, in an attempt to understand the deformation mechanisms that led to fracture.

2. Experimental procedure

Sheets, 1 mm thick, of this alloy were supplied by the Alcan Research Laboratories, Canada. The composition (wt %) was Ca 4.87, Zn 4.64, Fe 0.13, Si 0.09, Mg 0.01 and Al balance. (This composition, selected by Alcan Canada, represents an optimal compromise among good material properties, ease of production and high corrosion resistance.)

In order to obtain a microstructure similar to that present during superplastic flow, the as-received material was held at 540° C for 30 min and air cooled [2].

Tensile specimens with their longitudinal axis parallel to the rolling direction, and gauge dimensions 16 mm × 4 mm × 1 mm, were pulled to fracture on an Instron machine at constant cross-head speeds in the temperature range 275 to 550° C. The strain-rate sensitivity index, m, was determined as a function of temperature using a method that involves a change in cross-head speed [4]. The change in strain rate was by a factor of four as the cross-head speed was increased from 0.5 to 2.0 mm min^{-1}. (A small increase in strain rate does not alter the microstructure significantly when there is no change in the operating mechanism, and the assumption that m is independent of strain rate in the range employed is likely to be more realistic.) The general constitutive equation, $\sigma = K^*\varepsilon^n\dot{\varepsilon}^m$, where σ is the applied true stress, ε is the true strain, $\dot{\varepsilon}$ is the true strain rate, n is the strain-hardening coefficient and K^* is a material constant, was used to analyse the plastic flow behaviour in tension. Above 425° C, the simplified equation, $\sigma = K\dot{\varepsilon}^m$ was used (with K a constant), as it is known that in the absence of significant grain growth during deformation, strain hardening is absent in the region of optimal superplastic flow [4]. The variations in n and K^* with temperature were evaluated using the least squares method.

The fracture surfaces of tensile specimens tested at different temperature–strain rate combinations were carefully sectioned, cleaned ultrasonically in acetone solution and examined under the scanning electron microscope (SEM).

3. Results and discussion

3.1. Grain size

An etchant made from 45 ml HNO_3, 40 ml HF and 45 ml H_2O_2 was used to reveal the microstructure. The two-dimensional grain size of the second phase ($CaZnAl_3$) was 1.0 ± 0.5 μm. The matrix grains could not be fully revealed. The isolated parent phase grains that were visible were slightly larger in size (2 to 3 μm) than the second-phase particles. Fig. 1 shows a typical microstructure of the heat-treated Al–Ca–Zn alloy. The volume fraction of the second phase was approximately 20% [5].

0022–2461/90 $03.00 + .12

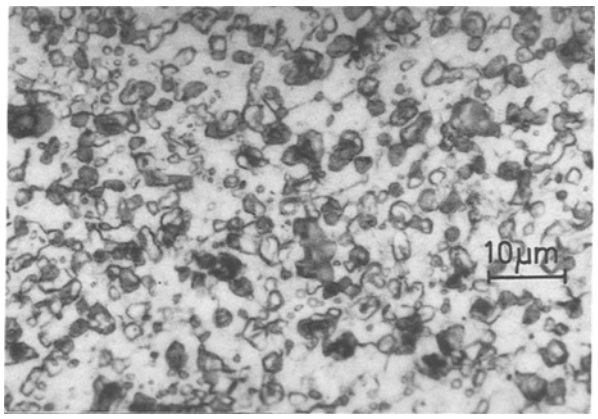

Figure 1 Microstructure of the Al–Ca–Zn alloy (after solution treatment at 540° C for 30 min and air cooling to room temperature).

3.2. Tensile flow behaviour in the range 275 to 550° C

The tensile properties of the alloy in the range 25 to 200° C were presented earlier [3]. Table I presents the tensile properties of the alloy in the range 275 to 550° C. In this range, yield-point elongation was not present. Nor was there a clear UTS, unlike in the lower temperature regime. The yield strength decreased with increasing temperature but was directly related to the strain rate (conventional behaviour). The fracture strain, e_f, increased with increasing temperature and decreasing strain rate (at a given temperature). Up to 425° C, m was determined by a strain-rate jump test. Beyond this temperature, however, jerky flow was present and an accurate determination of the steady state stresses at the two strain rates was not possible. Therefore, beyond 425° C, m was evaluated at a constant strain of 30% from the slope of the log true stress–log true strain rate plots in the strain rate range of 10^{-3} to $10^{-2}\,sec^{-1}$. At 550° C, the value of m was 0.35, which is in agreement with earlier results [1]. However, at 500° C the log true stress–log true strain rate plot was not linear and a mean line had to be drawn to obtain an m value of 0.23. This value is not realistic in view of the higher m value obtained at 425° C itself. So, for further analysis a value of 0.32 for m was taken from a smooth curve connecting the results pertaining to the other temperatures, i.e. the value was obtained by the method of interpolation.

True stress–true strain plots for different temperatures and strain rates are presented in Figs 2a to c. The arrow indicates the onset of "steady state" behaviour [6]. At the intermediate temperatures of 275 and 350° C strain hardening was absent. But beyond 425° C, however, marked strain hardening was seen. Similar "apparent strain hardening" is reported in the literature for other superplastic alloys and this has been attributed primarily to dynamic grain growth [7]. A microstructural study confirmed that in the present case also, the apparent strain hardening was caused by dynamic grain growth. A grain size of 2 to 3 μm before deformation had increased approximately to 4 to 6 μm after superplastic deformation. The microstructures showed two types of second-phase particles, which appeared dark or bright. Padmanabhan *et al.* [8] have established, using energy-dispersive analysis, that these corresponded to zinc-rich and calcium-rich particles, respectively. The $CaZnAl_3$ second-phase particles also experienced considerable grain growth from $1 \pm 0.5\,\mu m$ to approximately $3 \pm 0.5\,\mu m$. Qingling *et al.* [9] have reported a similar trend and have further noted that the average coarsening rate in the superplastic regime of the $CaZnAl_3$ intermetallic particles decreased with increasing volume fraction of the eutectic intermetallics. (Although a certain volume fraction of the intermetallic particles is essential for grain-size refinement and stability, coarse and columnar particles promote cavitation and impair superplasticity and hence their formation needs to be suppressed [9].)

For the superplastic 7475 Al alloy, Ghosh [7] has reported that for a given strain rate the hardening decreased significantly at higher temperatures. In the present study, however, two trends were found, i.e. for the lowest strain rate employed ($1.0 \times 10^{-3}\,sec^{-1}$), as the temperature increased, hardening decreased. But, at higher strain rates ($5.0 \times 10^{-3}\,sec^{-1}$ and $1.0 \times 10^{-2}\,sec^{-1}$) as the temperature increased hardening also increased. Secondly, Ghosh [7] has observed that at a given temperature, as the strain rate increased the hardening was more, instead of being less, which

TABLE I Al–Ca–Zn alloy – Mechanical properties in the range 275 to 550° C

Serial number	Temperature (° C)	Initial strain rate (sec^{-1})	Yield stress (MPa)	Fracture strain, e_f (%)	m (experimental)
1	275	1.0×10^{-3}	67.0	61.0	0.125
2		5.0×10^{-3}	70.2	66.0	
3		1.0×10^{-2}	72.0	57.0	
4	350	1.0×10^{-3}	22.1	84.0	0.225
5		1.0×10^{-2}	40.2	71.0	
6	425	1.0×10^{-3}	15.2	150.0	0.275
7		5.0×10^{-3}	17.7	122.0	
8		1.0×10^{-2}	25.7	91.0	
9	500	1.0×10^{-3}	11.8	255.0	0.320*
10		5.0×10^{-3}	15.8	200.0	
11		1.0×10^{-2}	21.3	178.0	
12	550	1.0×10^{-3}	10.9	306.0	0.350
13		5.0×10^{-3}	14.7	272.0	
14		1.0×10^{-2}	18.4	244.0	

*Determined by interpolation, see Section 3.2.

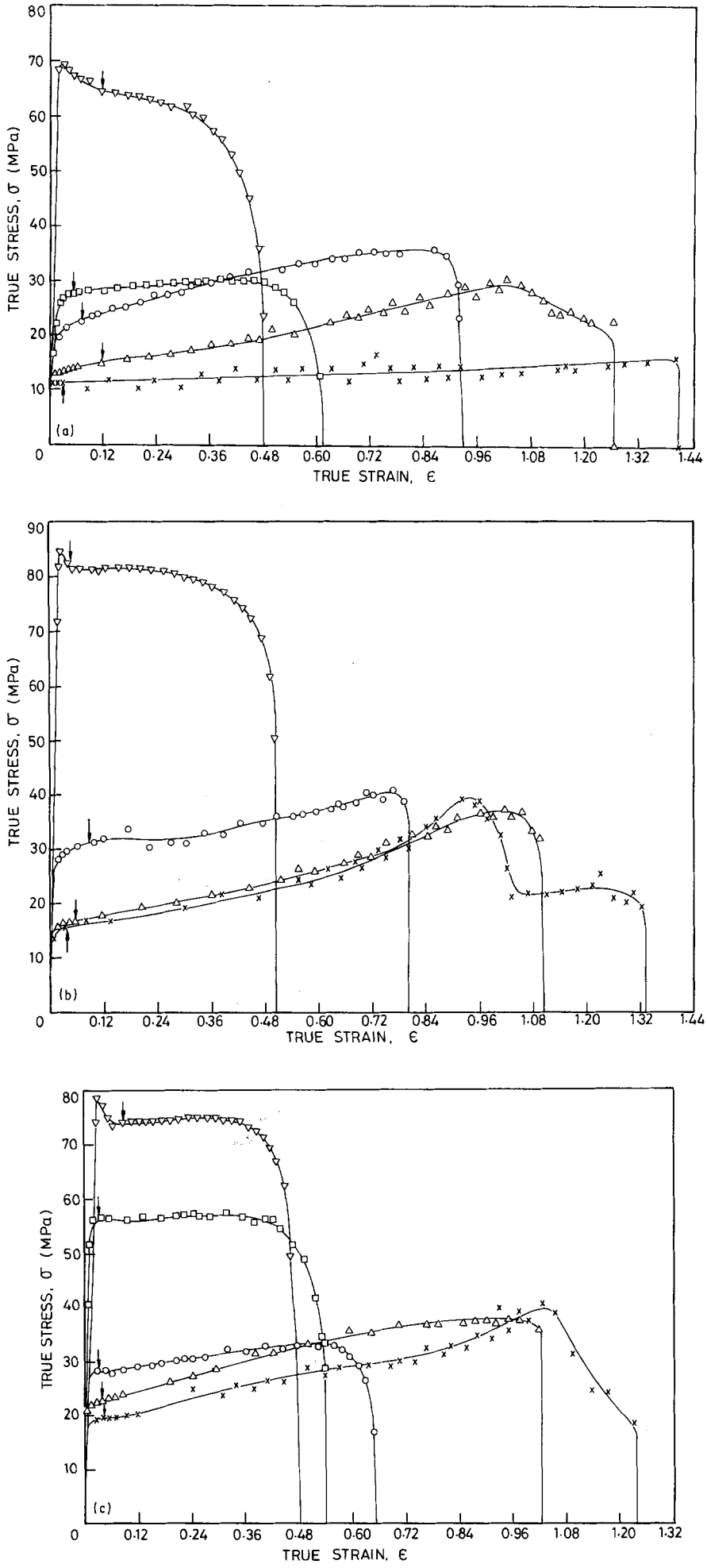

Figure 2 True stress–true strain plots of the Al–Ca–Zn alloy in the temperature range 275 to 550° C at an initial strain rate of (a) $1.0 \times 10^{-3}\,sec^{-1}$, (b) $5.0 \times 10^{-3}\,sec^{-1}$, and (c) $1.0 \times 10^{-2}\,sec^{-1}$. Temperature (° C): (▽) 275, (□) 350, (○) 425, (△) 500, (x) 550.

should have been the case if grain growth alone were responsible for the hardening (because less time is available for grain growth at the higher strain rates). In the present study, at higher strain rates the stress levels were clearly higher (due to the highly strain-rate sensitive flow) but the rate of hardening was not significantly affected except for the solitary temperature–strain rate combination of 550° C and 1.0×10^{-3} sec^{-1}, where hardening was found to be the least. Thirdly, Ghosh has cited microstructural evidence for the rate of dislocation accumulation in the grain interior being rapid enough to initiate dynamic recrystallization at the higher strain rates (or for a coarser initial grain size) and also a noticeable grain elongation (which could mean dislocation creep). In the present study, there was no evidence for either grain elongation or for dynamic recrystallization in the optimal range of superplastic flow.

Based on his observations concerning the 7475 Al alloy, Ghosh has argued that the evolution of the dislocation structure could also be contributing significantly to "apparent strain hardening" (apart from dynamic grain growth). Similar conclusions were reached by Ramirez *et al.* [10] in case of the Al–Ca–Zn alloy. However, based on our observations in the Al–Ca–Zn alloy reported here, taken together with those of Ghosh, the following alternative view to explain "apparent strain hardening" is proposed. In our view, the presently seen "apparent strain hardening" is essentially due to dynamic grain growth which increases with temperature. With increasing grain size, the grain-boundary area decreases and so resistance to deformation increases (in the superplastic range $\sigma \propto d^a$, where d is the grain size and a a positive constant). However, with increasing temperature the rates of grain-boundary deformation processes also increase, e.g. grain-boundary diffusivity. This will decrease the flow resistance of the material. Therefore, depending on which of the two effects (due to an increase in temperature) is dominating, strain hardening or softening could take place. This picture is able to account for both the opposing trends seen in the present study, whereas in the proposal of Ghosh both dynamic grain growth and recrystallization triggered by dislocation accumulation are necessary to understand the results. Nevertheless, it is noted that when the strain rate is very high, dislocation accumulation can lead to dynamic recrystallization. In the absence of experimental evidence, it has been felt unnecessary to invoke this additional process. (Please also see Section 3.3 for the effect of cavitation on apparent strain hardening.)

Fig. 3 shows some of the Al–Ca–Zn alloy specimens tested at elevated temperatures. The maximum elongation obtained was 306% at 550° C and strain-rate of 1.0×10^{-3} sec^{-1}. This value is low when compared with a published value of around 600% [5] and an unpublished figure of about 900% [2] for maximum ductility in this alloy. This low value could be traced to the specimen geometry (16 mm × 4 mm × 1 mm), as adequate material was not available for flow from the (long and short) transverse directions. (It may be noted in passing that when attempting to evaluate m at 550° C by the strain rate change test (although unsuccessfully, using specimen 12 in Fig. 3), the highest elongation of 400% was obtained. This suggests that the maximum elongation at 550° C can be increased by adopting slightly different strain rates from the ones used in this study.)

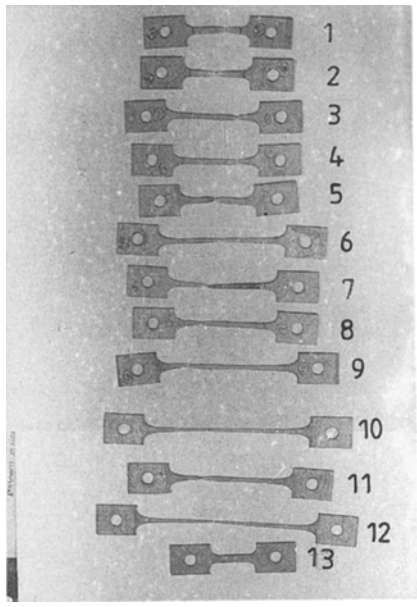

Figure 3 A photograph of some tested specimens of the Al–Ca–Zn alloy. Test conditions of temperature (° C), strain rate (10^{-3} sec^{-1}) for specimens (1) 350, 5.0; (2) 350, 10.0; (3) 425, 1.0; (4) 425, 5.0; (5) 425, 10.0; (6) 500, 1.0; (7) 500, 5.0; (8) 500, 10.0; (9) 550, 5.0; (10) 550, 1.0; (11) 550, 10.0; (12) 550, strain rate change test (maximum elongation of $\simeq$ 400%); (13) untested specimen.

Serrated flow was present at 500 and 550° C (in Figs 2a to c the zig-zag stress pattern is shown, but for clarity only a mean curve is drawn), similar to what was seen by Padmanabhan *et al.* [2]. Lloyd and Moore [5] have attributed the presence of serrated flow in a superplastic aluminium alloy to the presence of substitutional impurities like copper and magnesium. In commercial aluminium, Al–2 wt % Ge and Al–4 wt % Ge alloys serrated flow has also been reported. In commercial aluminium, iron and silicon atoms are considered to be responsible for serrated flow [11]. As the present alloy also contains appreciable amounts of iron (0.13 wt %) and silicon (0.09 wt %) and 0.01 wt % magnesium, one or more of these substitutional impurities could have been responsible for the serrated flow.

In Figs 2a to c it is also noted that at 500 and 550° C significant post-uniform elongation was present. An engineering strain of over 25% (up to a maximum of 35%) was present from the point of localized necking until failure. This is understandable in view of the large values of m under these conditions [4, 12].

Table II presents the calculated values of the strain-hardening coefficient, n, and the strength coefficient, K^*, for various experimental conditions based on a least squares analysis and the constitutive equation, $\sigma = K^* \varepsilon^n \dot{\varepsilon}^m$. The experimental values of the true stress, σ, true strain, ε, true strain rate, $\dot{\varepsilon}$, and m were used in the calculations. It is seen that at 275 and 350° C the values of both n and K^* lie in the physically meaningful range and also suggest a decreasing n

TABLE II Calculated values of n and K^* from the equation $\sigma = K^*\dot{\varepsilon}^n \circ \varepsilon^m$ using the least squares method

Serial number	Temperature (° C)	m (experimental)	Initial strain rate (sec^{-1})	n	K^* (MPa sec^m)
1	275	0.125	1.0×10^{-3}	0.031	144.9
2			5.0×10^{-3}	0.014	163.9
3			1.0×10^{-2}	0.034	142.5
4	350	0.025	1.0×10^{-3}	0.081	164.1
5			1.0×10^{-2}	0.046	182.9
6	425	0.275	1.0×10^{-3}	0.230	204.3
7			5.0×10^{-3}	0.223	205.3
8			1.0×10^{-2}	0.170	147.6
9	500	0.320*	1.0×10^{-3}	0.530	328.7
10			5.0×10^{-3}	0.437	218.3
11			1.0×10^{-2}	0.431	224.6
12	550	0.350	1.0×10^{-3}	0.435	230.1
13			5.0×10^{-3}	0.393	231.6
14			1.0×10^{-2}	0.371	215.9

*Determined by interpolation, see Section 3.2.

value with increasing temperature, which is in accordance with earlier results [3]. These results are noteworthy in view of the fact that both n and K^* were free to vary independently. In this analysis, beyond 425° C, n increased significantly and K^* also showed some increase. (Thus, the "apparent strain hardening" is also reflected in the numerical computations.) However, as n is low in the regime of optimal superplastic deformation (when grain coarsening is accounted for), the computations were repeated for the temperature range 425 to 550° C using the least squares procedure and a constitutive equation $\sigma = K\dot{\varepsilon}^m$, which best describes superplastic flow [3, 4]. The results of this computation are shown in Table III and the values of K obtained are again physically realistic.

3.3. Fracture behaviour in the range 275 to 550° C: uniaxial tension

Fig. 4 shows the fracture surface of a specimen tested at 275° C and a strain rate of $1.0 \times 10^{-3}\,sec^{-1}$. Large cavities interlinked by tear ligaments are prominent. A number of globular grains are seen inside the cavities and along the cavity walls. Wavy markings are frequently seen on the cavity surfaces. These could have resulted from wavy slip (or serpentine glide) occurring on a series of favourably oriented planes [13]. These are instances of the void surfaces being produced by the deformation traces associated with localized strain.

Figs 4b and c show the fracture surfaces of specimens tested at 350° C at strain rates of 1.0×10^{-3} and $1.0 \times 10^{-2}\,sec^{-1}$. The fracture surface is confined to the diagonal band (running from bottom left to top right) in Fig. 4b and is flanked on either side by the side walls of the specimen. The side walls are seen to be rumpled heavily, which implies significant grain-boundary sliding. In Fig. 4c the central horizontal portion represents the fracture surface and here the rumpling of the side walls is somewhat less (i.e. sliding becomes less important at the higher strain rate). Fractographs at higher magnifications (not shown here) revealed the alignment of a large number of cavities along the fracture surface and normal to the tensile axis, which were interlinked by thin tear ligaments.

Figs 4d and e show two interesting fractographs of specimens pulled to failure at 425° C at strain rates of 1.0×10^{-3} and $1.0 \times 10^{-2}\,sec^{-1}$, respectively. Sudden failure appears to have taken place through extensive slip across the specimen thickness. At the higher strain rate, catastrophic shear by rapidly propagating intersecting shear instability bands from opposite sides has apparently prevented the occurrence of cavity-interlinked failure. The fracture surface has accordingly taken a sharp, wedge-like and an entirely featureless appearance (even at a high magnification of × 1200). The following speculation on this aspect seems reasonable.

From 25 to 350° C, transcrystalline, dimple-type failure was evident. At test temperatures above 425° C (i.e. at 500 and 550° C), where superplastic ductility is seen, grain-boundary deformation processes, in

TABLE III Calculated values of K from the equation $\sigma = K \circ \varepsilon^m$ using the least squares method

Serial number	Temperature (° C)	m (experimental)	Initial strain rate (sec^{-1})	K (MPa sec^m)
1	425	0.275	1.0×10^{-3}	222.9
2			5.0×10^{-3}	162.5
3			1.0×10^{-2}	119.1
4	500	0.32*	1.0×10^{-3}	237.2
5			5.0×10^{-3}	148.8
6			1.0×10^{-2}	172.5
7	550	0.35	1.0×10^{-3}	212.8
8			5.0×10^{-3}	156.6
9			1.0×10^{-2}	156.0

*Determined by interpolation, see Section 3.2.

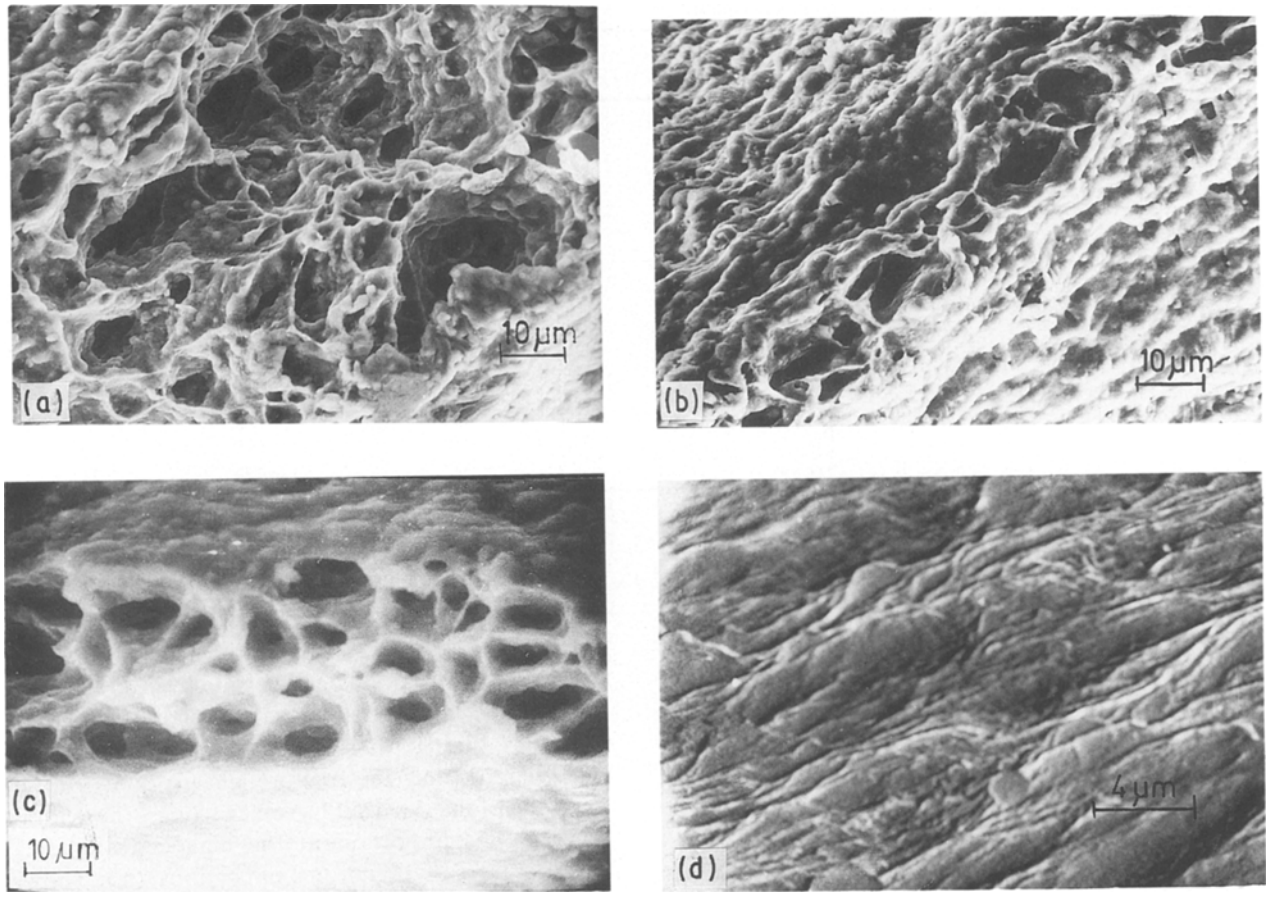

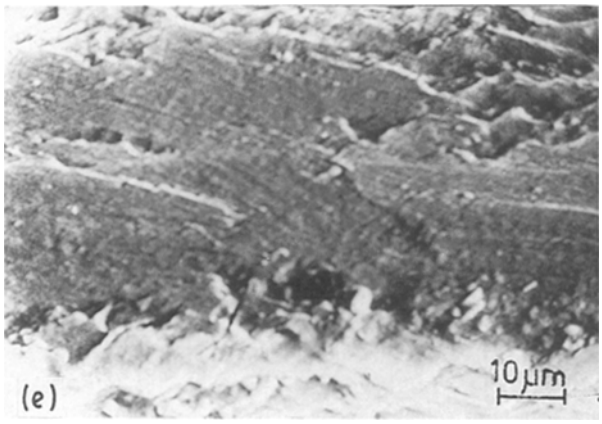

Figure 4 Some typical fractographs of specimens of the Al–Ca–Zn alloy tested in the non-superplastic regime. Temperature (° C) and strain rate (sec^{-1}) were: (a) 275, 10^{-3}; (b) 350, 10^{-3}; (c) 350, 10^{-2}; (d) 425, 10^{-3}; (e) 425, 10^{-2}.

particular grain-boundary sliding, become dominant and influence the deformation up to failure. Therefore, the specimen cross-section decreases considerably without failure, and features such as large cavities are tolerated because of the enhanced strain-rate sensitivity (m value) of the material at these temperatures, which imparts high necking resistance to inter-cavity ligaments [4]. In the vicinity of 425° C, the deformation mechanism appears to undergo a transition from grain-deformation control at the lower temperatures to grain-boundary deformation processes (chiefly sliding) at the higher temperatures. In this transition range, the m value, although high, is still only about 0.27. Therefore, when a critical reduction in cross-section takes place, the deformation does not shift quickly elsewhere, in spite of an increase in the local strain rate. That is, the formation of diffuse necks (characteristic of superplastic flow) is not yet obvious. Under these conditions the material fails by catastrophic shear, being unable to support the load any further. Consistent with this idea, the maximum elongation at 425° C was only 150% and this can only be termed as extended plasticity.

Figs 5a and b show fractographs corresponding to specimens pulled to failure at 500° C at strain rates of 1.0×10^{-3} and $1.0 \times 10^{-2}\,sec^{-1}$, respectively. The former picture shows large deep cavities along with numerous clusters/clumps of grains. Cavity interlinkage is through transcrystalline as well as inter-cavity ligaments. In the latter figure, pronounced rumpling of the side walls is seen which indicates the dominant role of grain-boundary sliding in deformation at this temperature [4].

Figs 5c and d display the fracture surfaces of specimens tested to failure at 550° C at strain rates of 1.0×10^{-3} and $1.0 \times 10^{-2}\,sec^{-1}$, respectively. In Fig. 5c the fracture surface has thinned down to wedge-like sharpness with large cavities on either side. (This corresponded to the maximum ductility of 306% obtained in this study for this alloy.) In Fig. 5d (a higher strain rate), cavities are seen to be smaller and the tear ridges thicker, which is understandable in view of the lower ductility (compared with the previous case).

Table IV gives a quantitative correlation between the fracture behaviour and the ductility of the alloy in terms of the average cavity size (in the fracture face) and the fracture strain. Cavity size increased with an

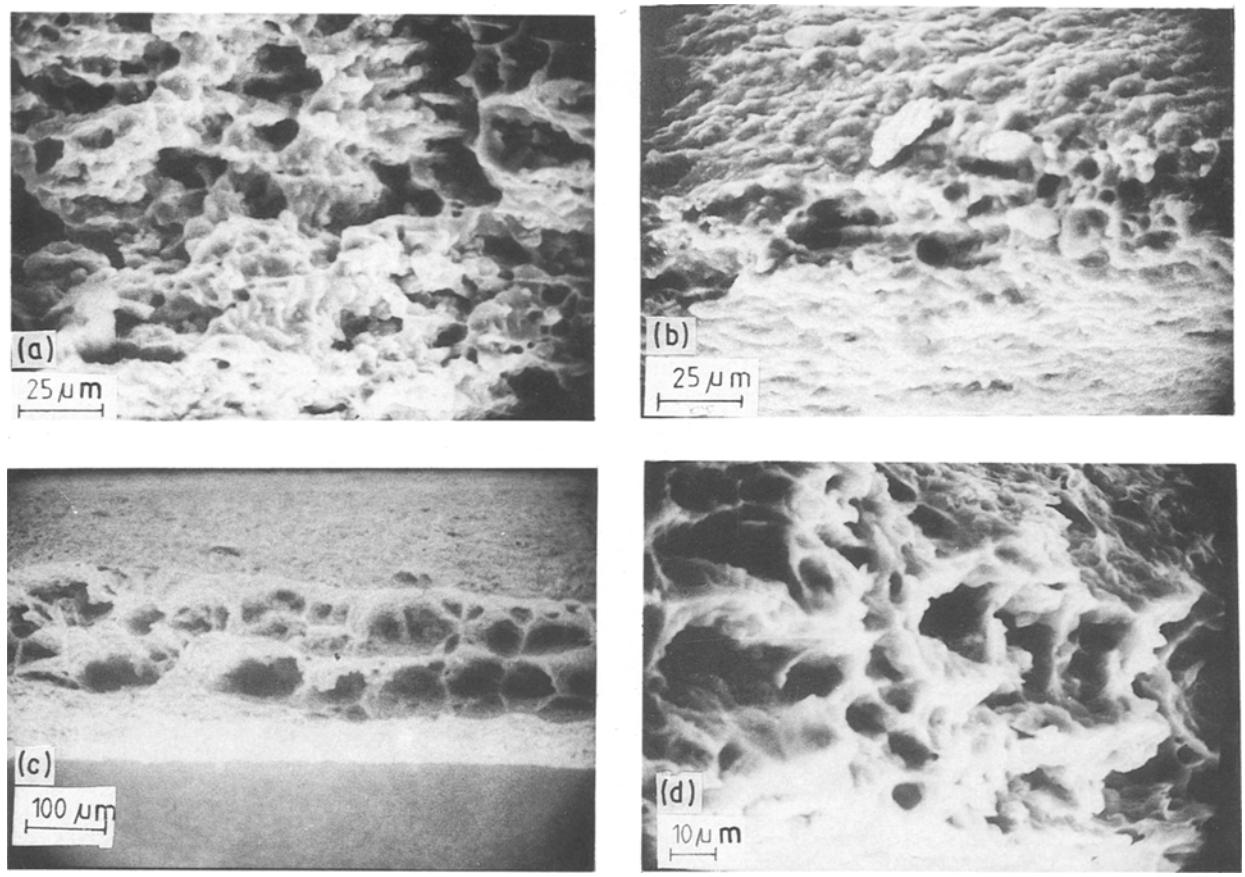

Figure 5 Fractographs of specimens of the Al–Ca–Zn alloy tested in the superplastic regime. Temperature (° C) and strain rate (sec^{-1}) were: (a) 500, 10^{-3}; (b) 500, 10^{-2}; (c) 550, 10^{-3}; (d) 550, 10^{-2}.

increase in temperature; a greater increase was associated with a lower strain rate. (Both are reasonable as the value of m and hence the ductility increased with increasing temperature or decreasing strain rate). However, it was obvious that even at a fixed temperature the cavity size changed with strain rate, indicating its critical dependence on the elongation at fracture. This observation perhaps suggests that cavity growth is plasticity dominated.

The extensive cavitation seen is considered to contribute in two ways to the "apparent strain hardening" discussed earlier (Section 3.2): (a) the presence of a large volume fraction of cavities invalidates the assumption of volume constancy in the calculation for determining the true stress, and (b) as the temperature increases, the m value also increases and this increases the internal necking resistance of the inter-cavity ligaments. Then, not only the tendency for tearing is reduced but also the flow stress level prior to failure is increased.

4. Conclusions

1. In the temperature range 200 to 550° C, the fracture strain of the superplastic Al–Ca–Zn alloy increased with temperature, the increase being steep above 400° C. Superplastic ductility could be seen at and above 500° C. The strain-rate sensitivity index, m, increased to a maximum value of 0.35 at 550° C.

2. Above 400° C, serrated flow was seen. Also, an appreciable post-uniform elongation (25% to 35%) was obtained due to the high value of the strain-rate sensitivity index at these temperatures.

3. In the true stress–true strain plots, marked strain hardening was apparent above 400° C. This "apparent hardening" under superplastic conditions was traced (using microstructural and fractographic results) to dynamic grain growth and extensive cavitation (which invalidated the assumption of volume constancy).

4. An analysis based on the method of least squares to determine the variation of the strain-hardening coefficient, n, and the strength coefficient, K^*, with

TABLE IV Average cavity size for different temperature–strain rate combinations. Temperature range 275 to 550° C

Temperature (° C)	Average cavity size (μm) (initial strain rate $1.0 \times 10^{-3}\ sec^{-1}$)	Fracture strain, e_f (%)	Average cavity size (μm) (initial strain rate $1.0 \times 10^{-2}\ sec^{-1}$)	Fracture strain, e_f (%)
275	10.8	61.0	8.9	57.0
350	12.6	84.0	10.1	71.0
425	*	150.0	*	91.0
500	17.8	255.0	12.3	178.0
550	65.9	306.0	14.6	244.0

*Catastrophic slip failure; no cavities present.

temperature yielded fairly reasonable estimates for the temperature range 275 to 550° C.

5. SEM fractography resulted in a meaningful quantitative correlation between the average cavity size and the fracture strain in the range 275 to 550° C. The cavity size increased with temperature; at a given temperature, it was smaller for a higher strain rate. These results could be understood in terms of the changes in the value of m with temperature and strain rate and the fact that cavity growth is plasticity dominated.

6. Fractography revealed a transition in the dominant deformation mechanism from grain-deformation processes (mainly slip) to grain-boundary deformation processes (mainly grain-boundary sliding) in the vicinity of 425° C.

Acknowledgements

The authors thank Dr D. M. Moore, Alcan Laboratories, Canada, for supplying the Al–Ca–Zn alloy sheets used in this study, Dr P. Rama Rao for kindly permitting the use of the Instron testing machine, and Dr P. Rodriguez for permitting the use of the scanning electron microscope.

References

1. D. M. MOORE and L. R. MORRIS, *Mater. Sci. Engng* **43** (1980) 85.
2. K. A. PADMANABHAN, J. HIRSCH and K. LUCKE, unpublished work (1987).
3. P. P. DATE, K. SWAMINATHAN and K. A. PADMANABHAN, *J. Mater. Sci.* **23** (1988) 1351.
4. K. A. PADMANABHAN and G. J. DAVIES, "Superplasticity" (Springer Verlag, Berlin, Heidelberg and New York, 1980).
5. D. J. LLOYD and D. M. MOORE, in Proceedings of the Conference on "Superplastic Forming of Structural Alloys", edited by N. E. Paton and C. H. Hamilton, Metallurgical Society AIME, San Diego, 21–24 June (1982) (Metal Society AIME, Warrendale, Pennsylvania, 1982) pp. 161, 152.
6. R. K. YADAVA and K. A. PADMANABHAN, *Mater. Sci. Engng* **37** (1979) 127.
7. A. K. GHOSH, in Proceedings of the Symposium on "Superplastic Forming", edited by S. P. Agrawal, American Society for Metals, Los Angeles Chapter, California, March (1984) (American Society Metals, Metals Park, Ohio, 1985) p. 147.
8. K. A. PADMANABHAN, O. ENGLER, J. HIRSCH and K. LUCKE, personal communication (1988).
9. W. QINGLING, M. HONGSEN and M. LUNGXIANG, in Proceedings of the Conference on "Superplasticity in Aerospace Aluminium", edited by R. Pearce and L. Kelly, Cranfield, UK, July (1985) (Ashford Press, Curdridge, England, 1985) p. 168.
10. P. RAMIREZ, F. G. ALDAY, H. E. ADABBO and O. A. RUANO, *Mater. Sci. Engng* **93** (1987) L11.
11. A. M. HAMMAD, PhD thesis, Institute of Technology, Banaras Hindu University (1978).
12. A. K. GHOSH, *Trans. Amer. Soc. Met.* **99** (1977) 264.
13. R. H. VAN STONE, T. B. COX, J. R. LOW Jr and J. A. PSIODA, *Int. Metall. Rev.* **30** (1985) 157.

Received 26 April
and accepted 29 November 1989